Ergodicity-Based Cooperative Multiagent Area Coverage via a Potential Field

Stefan Ivić, Bojan Crnković, and Igor Mezić

***Abstract*—This paper considers a problem of area coverage where the objective is to achieve given coverage density by use of multiple mobile agents. We present an ergodicity-based coverage algorithm which enables a centralized feedback control for multiagent system based on radial basis function (RBF) representation of the ergodicity problem and a solution of an appropriately designed stationary heat equation for the potential field. The heat equation uses a source term that depends on the difference between the given goal density distribution and the current coverage density (time average of RBFs along trajectories). The agent movement is directed using the gradient of that potential field. The heat equation driven area coverage has a built-in cooperative behavior of agents which includes collision avoidance and coverage coordination. The algorithm is robust, scalable, and computationally inexpensive.**

***Index Terms*—Area coverage, cooperation, ergodicity, feedback control, heat equation, multiagent system.**

I. Introduction

THE MULTIAGENT area coverage problem is one of the most challenging problems emerging from rapid advancement in autonomous mobile agents industry. Unmanned vehicles—ground, aerial, water surface or underwater—are used to perform a variety of actions on the area of interest. The use of multiagent systems in problems like area coverage has obvious advantages over single agent coverage, but also raises some problems like cooperation, collision and a potential deadlock of agents that need to be considered. This paper considers the problem of area coverage using such a system of cooperative agents.

There are two basic types of coverage problems that are considered in recent papers. The first type is a static coverage problem where the task is to find an optimal static configuration of sensors that fit the goal stationary probability distribution. The second is a problem of dynamical coverage accomplished by continuous movement of agents in order to achieve given goal coverage density. In addition to the above classification, area search problems with target detection and path finding are related to area coverage problem and are solved with similar methods and techniques.

Coverage, search or path finding problems are also considered as an optimization problem with the task of finding optimal trajectories in respect to various objectives and constraints. The foundations and basic theory of optimal search with target detection can be found in [20]–[22] and [36].

Spanning tree covering [12] is a cellular automata-based coverage method where agent uses its sensors to detect obstacles and construct a spanning tree of the environment while covering the work-area. A similar approach in [31] uses a coverage tree that can accommodate nonuniform coverage of regions in the target area.

The algorithms presented in [8] exploit the computational geometry of spatial structures such as Voronoi diagrams. The discussed method is extended to provide an optimal stationary coverage for time-varying distribution density function. A dynamic coverage control algorithm is proposed in [15] which only requires a finite number of messages to be exchanged among the agents and guarantees coverage of convex polygonal area in finite time.

Potential field approach is widely used for planning of mobile agents' motion and the distribution of stationary sensors because of its simplicity and elegance. Several approaches based on potential fields are used for coverage, search, path planing or related methods for both static and dynamic problems. A potential-field-based approach is used for path planning [38], sensor deployment [16], and exploration of an unknown environment [30]. A more advanced approach, using a Laplace equation to model the potential field, is utilized in [9], [25], [32], and [33].

Combination of potential field and Voronoi diagrams approach, together with visibility graph technique, is used in [24] to solve a path planning problem. Receding horizon control method [4], [5] is used to find optimal trajectories that maximize spatial coverage in a given time interval.

Partitioning or decomposition of the domain, as a technique in area search or coverage problems, is investigated in several papers. A survey of early researches on cellular domain decomposition is given in [7]. Domain decomposition is extended and combined with optimal path planning in [6] and adaptive task allocation in [29]. Area search method in [39] dynamically partitions the search area based on the target density distribution. Domain partitioning accounts for

Manuscript received April 28, 2016; revised August 23, 2016 and November 19, 2016; accepted November 29, 2016. Date of publication December 16, 2016; date of current version July 17, 2017. This work was supported in part by the University of Rijeka through the Environmental Modeling in the Coastal Region of Rijeka Bay 13.09.1.2.12, and in part by the AFOSR under Grant FA9550-12-1-0230. This paper was recommended by Associate Editor X.-M. Sun.

S. Ivić is with the Faculty of Engineering, University of Rijeka, 51000 Rijeka, Croatia (e-mail: stefan.ivic@riteh.hr).

B. Crnković is with the Department of Mathematics, University of Rijeka, 51000 Rijeka, Croatia.

I. Mezić is with the Department of Mechanical Engineering, University of California at Santa Barbara, Santa Barbara, CA 93106 USA.

This paper has supplementary downloadable multimedia material available at http://ieeexplore.ieee.org provided by the authors.

Digital Object Identifier 10.1109/TCYB.2016.2634400

regions of potential targets with varying levels of uncertainty. An algorithm based on cellular decomposition is used for complete-coverage of unstructured environments [1], [2], [13].

A method for carrying out a long endurance area surveillance missions is presented in [3]. The emphasis of this method is put on cooperation of agents realized by "one-to-one" coordination which ensures to get a near optimal solution keeping a periodic information interchange between all agents. A search strategy presented in [19] is also focused on cooperation of search agents. The information merging strategy is used for occupancy and data exchange between agents.

A cooperative multiagent search method is used in [40] for target search in uncertain environment. It uses a decentralized strategy based on sensor reading and data obtained trough the search. Combination of local and global strategies to achieve efficient multiagent coverage and bounded repulsive avoidance control law for collision avoidance is presented in [11]. The local agent guidance strategy is based on the gradient of local coverage error. A control strategy based on variable coverage action and variable coverage range of the agents is proposed in [10]. Reduction of coverage error and energy consumption is achieved with adaptive behavior in terms of actuator power and actuator domain.

The spectral multiscale coverage (SMC) [17], [26], [27] approach provides a centralized feedback control laws for multiagent systems so that agents trajectories sample a given distribution of target locations as uniformly as possible. The method was applied to dynamic area search problem in [28] and to adaptive search in [37]. It uniquely sets the problem as the one of weak convergence of the delta distribution on agent trajectories to the prescribed distribution that is often absolutely continuous with respect to Lebesgue measure. The SMC algorithm is based on the idea that agent trajectories should be ergodic with respect to the prescribed measure. This leads to the formulation of the method in terms of a scaled difference of spectral transforms of coverage and goal fields. Use of the Fourier transform in the SMC algorithm can be computationally demanding and in some special cases cause instability in agent movement. Due to the choice of the global Fourier basis, the method tends to perform global coverage first and later focuses on local coverage. In some applications, it is more advantageous to explore the local area first. Furthermore, in SMC, excessively covered areas can cause suboptimal behavior of agents.

In [18], dynamical covering for partially connected mobile agents with guaranteed collision avoidance is introduced. The model presented in [18] was used to obtain decentralized coverage control in [34].

We present a new method which is able to carry out a cooperative and synchronized multiagent movement with a task to achieve targeted spatial area coverage, focusing on local exploration. This is achieved by first formulating the ergodicity problem in terms of—local—radial basis functions (RBFs) and formulating a "smoothed gradient potential field" control method to minimize the error between the delta measure on trajectories and the prescribed measure. Both smoothing of the gradient and collision avoidance (that is not built into the basic SMC method) are achieved using a heat equation formulation. Thus, our approach combines ideas used in the SMC methods and methods based on potential field theory.

II. Area Coverage Controlled by Heat Equation

In this consideration, we generalize action performed by agents and focus on the agents motion control in order to provide effective area coverage.

Although real coverage problems are mainly 2-D, the proposed method could be applied to multidimensional problems. Thus, the coverage problem formulation and the definition of proposed method considers n-dimensional multiagent coverage.

A. Area Coverage Problem Formulation

The multiagent coverage algorithm presented in this paper is based on a centralized control of agents motion in the bounded n-dimensional domain $\Omega \subset \mathbb{R}^n$ with a Lipschitz continuous boundary. For now, let us consider trajectories of mobile agents as known and are denoted by $\mathbf{z}_i : [0, t] \to \mathbb{R}^n$, for $i = 1, 2, \ldots, N$ where N is the number of mobile agents.

Consider a positive smooth local RBFs ϕ and ϕ_σ that satisfy

$$\phi_\sigma(\mathbf{x}) = \sigma^{-n}\phi\left(\frac{\mathbf{x}}{\sigma}\right) \tag{1}$$

$$\int_{\mathbb{R}^n} \phi(\mathbf{x})\, \mathrm{d}\mathbf{x} = 1 \tag{2}$$

where σ is a positive scaling factor.

With known agent trajectories, the coverage density at time t can be defined as

$$\tilde{c}_\sigma(\mathbf{x}, t) = \frac{1}{N t} \sum_{i=1}^{N} \int_0^t \phi_\sigma(\mathbf{x} - \mathbf{z}_i(\tau))\, \mathrm{d}\tau. \tag{3}$$

The coverage density can be seen as the time average along trajectories $\mathbf{z}_i(\tau)$ of a function $\phi_\sigma^{\mathbf{x}}$

$$\phi_\sigma^{\mathbf{x}}(\mathbf{y}) = \phi_\sigma(\mathbf{x} - \mathbf{y}).$$

The functions $\phi_\sigma^{\mathbf{x}}$ can be seen as a family of functions in $L^2(\Omega)$, parameterized by the spatial point $\mathbf{x}$. In the current formulation, they replace the Fourier basis used in the formulation of the SMS algorithm [27].

According to (3) the coverage is normalized in $\mathbb{R}^n$, but in the bounded domain Ω where the RBF support might be outside of the domain (near the boundary) (3) does not guarantee normalized coverage. Therefore, we need to use normalized coverage density (coverage in short)

$$c_\sigma(\mathbf{x}, t) = \frac{\tilde{c}_\sigma(\mathbf{x}, t)}{\int_\Omega \tilde{c}_\sigma(\mathbf{x}, t)\, \mathrm{d}\mathbf{x}}. \tag{4}$$

We want to control the motion of agents in order to achieve for their coverage c_σ to converge in some sense to the given goal density $m : \Omega \to \mathbb{R}$, where $\int_\Omega m(\mathbf{x})\, \mathrm{d}\mathbf{x} = 1$. Goal density m can be interpreted as a relative density of agents action over the domain Ω or as a probability density function.

The coverage c_σ depends on the selected radial function ϕ_σ. Obviously, since trajectories are 1-D, it would typically

take a Peano-curve type complicated construct to achieve convergence of c_σ to a smooth goal density m as time goes to infinity. We relax the convergence requirement, moving to weak convergence of the delta distribution on agent trajectories $\langle 1/(N\,t)\sum_{i=1}^{N}\int_0^t \delta(\mathbf{x}-\mathbf{z}_i(\tau))\,\mathrm{d}\tau, \phi_\sigma\rangle = \tilde{c}_\sigma$ tested on the space of RBFs to the prescribed distribution m as in SMC—and ask that the time average of $\phi_\sigma^{\mathbf{x}}$ matches its spatial average with respect to m

$$(\phi_\sigma * m)(\mathbf{x}) = \int_{\mathbb{R}^n} \phi_\sigma(\mathbf{y}) m(\mathbf{x}-\mathbf{y})\,\mathrm{d}\mathbf{y} = \int_{\mathbb{R}^n} \phi_\sigma^{\mathbf{x}}(\mathbf{z}) m(\mathbf{z})\,\mathrm{d}\mathbf{z} \tag{5}$$

where in the last equality we used the property $\phi_\sigma(\mathbf{z}) = \phi_\sigma(-\mathbf{z})$ of RBF. The term $\phi_\sigma * m$ represents the spatial diffusion of the goal density m. We define a local error as difference between goal and coverage density

$$e(\mathbf{x}, t) = (\phi_\sigma * m)(\mathbf{x}) - c_\sigma(\mathbf{x}, t). \tag{6}$$

The scalar field e is a spatial distribution of error, where negative and positive values indicate insufficiently and excessively covered areas, respectively.

The error estimate E is defined as L_2 norm of the local error field e

$$E(t) = \|e(\mathbf{x}, t)\|_2. \tag{7}$$

$E(t)$ can be considered as global error which is used to evaluate overall area coverage success for given agent trajectories. It can be evaluated at any time to monitor the convergence of the coverage process. As we want to minimize the difference between goal density and coverage density, the objective of the area coverage method is to achieve

$$\lim_{t\to\infty} E(t) = 0. \tag{8}$$

If this is satisfied, we say that trajectories of the multiagent system are *ergodic* [27]. The agent trajectories are continuous, their speed is bounded and they cannot jump from one place in the domain to another, therefore $E(t)$ cannot in general be a monotonically decreasing function of t. The main task of the coverage method is to define a rule for movement of mobile agents that will ensure that the error will decrease for a large enough time t and (8) can be achieved.

B. Agent Motion Control

Control of agents' motion can be accomplished in several ways, where different physical or technical limitations of real agents can be considered. A simple control of agent movement can be achieved with kinematic or dynamic model, represented with first and second order differential equations, respectively. For more realistic and accurate mobile agent movement, a more detailed vehicle, plane or helicopter model can be used.

To keep the focus on the problem of coverage efficiency and agent cooperation, we choose the simplest first order kinematic model that neglects agent mass and inertia. Using this model, there is no need to deal with agent behavior near the edge of the domain or similar issues which arise when using more complex models.

In the kinematic model, our ansatz for the movement of agents is

$$\frac{\mathrm{d}\mathbf{z}_i(t)}{\mathrm{d}t} = v_a \cdot \frac{\nabla u(\mathbf{z}_i(t), t)}{||\nabla u(\mathbf{z}_i(t), t)||}, \quad i = 1, \ldots, N \tag{9}$$

with initial conditions

$$\mathbf{z}_i(0) = \mathbf{z}_{i,0}, \quad \mathbf{z}_{i,0} \in \Omega, \quad i = 1, \ldots, N \tag{10}$$

where v_a is the maximum agent velocity and $u : \mathbb{R}^{n+1} \to \mathbb{R}$ is a scalar field that we will define below. While the magnitude of agent velocity is constant and equal for all agents, the direction of the agent depends on current position of the agent and the gradient of scalar field u. Since we want to minimize the error E, the field u will be related to the spatial error distribution (6).

At first sight, $u = e$ might look like a good choice to minimize the error, but due to different scales of spatial error and the presence of local minima it is not applicable in the present form for the global minimization of overall error E. The gradient of the error field e, cannot provide information of distant insufficiently covered areas in Ω. Furthermore, using the gradient of e, even local minimization is not guaranteed, since a zero gradient of e can be encountered. A similar issue was confronted in [11] where additional global control strategy was deployed.

To prevent these problems, we use the stationary heat equation, with proper boundary conditions, as a smoothing operator for the spatial error field e. As we show later, this is quite similar to using a modified norm (a negative Sobolev space norm, as in SMC) to capture weak convergence. In our construction, a modified local error field participates as a source of heat—which indicates insufficiently covered area—in the stationary heat equation. The heat conduction phenomena within the heat equation propagates information on the insufficiently covered area, as temperature, throughout the whole domain. The heat equation was the first diffusion process that was applied to digital images [35], where it was used to introduce a scale space to detect important features of the image.

The field u is obtained as a solution to the stationary heat equation defined as a partial differential equation

$$\alpha \cdot \Delta u(\mathbf{x}, t) = \beta \cdot u(\mathbf{x}, t) + \gamma \cdot a(\mathbf{x}, t) - s(\mathbf{x}, t) \tag{11}$$

with the boundary condition

$$\frac{\partial u}{\partial \mathbf{n}} = 0, \text{ on } \partial\Omega \tag{12}$$

where Δ is a Laplace operator, $\mathbf{n}$ is the outward normal, a is the sink, s is the source, and $\alpha > 0$, $\beta > 0$, and $\gamma \geq 0$ are tunable parameters that are explained below.

We introduce a non-negative spatial field

$$\tilde{s}(\mathbf{x}, t) = \max(e(\mathbf{x}, t), 0)^2 \tag{13}$$

which emphasizes the insufficiently covered areas and neglects the negative values of e (indicating oversampled areas). A similar modification of the error function is used in [18].

For convenience, $\tilde{s}$ is appropriately scaled

$$s(\mathbf{x}, t) = \frac{\tilde{s}(\mathbf{x}, t)}{\frac{1}{|\Omega|}\int_\Omega \tilde{s}(\mathbf{x}, t)\,\mathrm{d}\mathbf{x}}. \tag{14}$$

Using s as a heat source, a stationary heat equation is employed to produce a temperature field gradient which will lead agents to the areas of interest.

In the formulation (11), the diffusion term $\alpha \cdot \Delta u$ can be physically interpreted as heat conduction. The parameter α presents the thermal diffusivity which regulates the strength of the smoothing of the potential field by conduction. A stronger heat conduction, caused by choosing larger α, extends the range of influence of the heat (error) source in the domain and it is suitable to enhance global coverage control.

The term βu in (11) presents a convective heat flow and, in this case, governs cooling over the whole area of the domain. This is a special case of convective heat flow that can be written as $\beta(u-u_\infty)$, where u_∞ is the environmental temperature and β is convective heat transfer coefficient. Since the source s is always being non-negative, thus consistently acting as heating source, a convective heat flow βu tends to lower the temperature toward $u_\infty = 0$ and it can be regarded as cooling term. Overall heating and cooling heat flows are balanced when equilibrium temperatures u are reached. When increasing convective cooling, temperature field u tends to have more similar shape to source field s so details of uncovered areas are better emphasized in u. Thus, enlarging β leads to better local coverage.

The term $\gamma \cdot a$ represents local cooling generated at the agent positions. Field a is rescaled to be aligned with s

$$a(\mathbf{x}, t) = \frac{\tilde{a}(\mathbf{x}, t)}{\frac{1}{|\Omega|}\int_\Omega \tilde{a}(\mathbf{x}, t)\, \mathrm{d}\mathbf{x}} \tag{15}$$

where $\tilde{a}$ is agents cooling defined as the sum of RBFs centered on each agent's current position

$$\tilde{a}(\mathbf{x}, t) = \sum_{i=1}^{N} \phi_{\sigma_a}(\mathbf{x} - \mathbf{z}_i(t)). \tag{16}$$

Local cooling (16) is introduced to provide local repulsion effect between agents which enables better cooperative coverage and collision avoidance. It should be noted that this mechanism of collision avoidance does not guarantee minimal distance between agents. Guaranteed collision avoidance could be accomplished using a repulsive forces as presented in [18]. The influence of local cooling on the coverage process is regulated with two parameters: 1) the cooling intensity γ in (11) and 2) the cooling range σ_a in (16). The intensity of agents cooling can be interpreted as strictness of collision avoidance while σ_a is proportional to safety distance.

The Neumann boundary condition (12), in terms of heat equation, represents an ideal heat insulation on the edge of the domain. Insulation is an appropriate boundary condition because it prevents agents from leaving the domain, disables the heat flux trough the boundary and it ensures that agent motion is dominated by the properties of the heat source and not by the boundary conditions.

Note that for an efficient area coverage method, coefficients β and γ should not be constant if a change in the domain of the coverage problem is introduced. Specifically, if the coverage problem is spatially scaled, for example if different units are used, the solution of the stationary heat equation (11) would also change if β and γ stay constant. This issue can be simply resolved by scaling β and γ with the rate of the domain area change. Specifically, a unit domain $[0, 1]^2$ coefficients β_0 and γ_0 are used to calculate β and γ, respectively, based on the following simple scaling:

$$\begin{aligned} \beta &= \frac{\beta_0}{|\Omega|} \\ \gamma &= \frac{\gamma_0}{|\Omega|} \end{aligned} \tag{17}$$

where $|\Omega|$ is the area of the domain.

The proposed area coverage algorithm is a coupled system of ordinary differential equations (9) and the partial differential equation (11). The coupling is achieved by agents trajectories acting on the source therm of the heat equation and by temperature field gradient which directs the agents. The coupled system can be written as

$$\begin{aligned} \frac{\mathrm{d}\mathbf{z}_i}{\mathrm{d}t} &= v_a \cdot \frac{\nabla u(\mathbf{z}_i)}{||\nabla u(\mathbf{z}_i)||}, \quad i = 1, \ldots, N \\ \alpha \cdot \Delta u &= \beta \cdot u + \gamma \cdot a(\mathbf{z}_i) - s(\mathbf{z}_i) \end{aligned} \tag{18}$$

with corresponding initial (10) and boundary (12) condition.

According to [23], for $\gamma > 0$ the solution of (11) is unique, bounded and smooth if the data and boundary satisfy some regularity conditions. If the boundary $\partial\Omega$ is a C^2 surface and $s \in C^0(\Omega)$ then (11) has a unique solution $u \in C^2(\Omega)$. If the boundary $\partial\Omega$ is only Lipschitz continuous in a convex bounded domain Ω, like the ones used later in numerical test, with $s \in L_2(\Omega)$ then according to [14] there is a unique solution to (11) in Sobolev space $H^2(\Omega)$. Under reasonable assumptions on smoothness, gradient of u exists for all points of the domain Ω.

III. Comparison With SMC

SMC algorithm uses a negative Sobolev space metric that quantifies how far trajectories of agents are from being ergodic with respect to a given probability measure. This provides—on the surface—a different setting than the algorithm presented in this paper but it is possible to interpret the SMC algorithm in terms of coverage density functions. Using this metric, the centralized feedback control is designed so that agents trajectories sample a given probability distribution as uniformly as possible. SMC also considers a multidimensional coverage problem.

A. Spectral Multiscale Coverage

Although in [26] both first and second order dynamics for agent movement are used in SMC, we consider only the kinematic model for proper comparison with heat equation driven area coverage (HEDAC). The movement of an agent is governed by the first order differential equation where ith agent velocity is obtained similarly to (9)

$$\frac{\mathrm{d}\mathbf{z}_i}{\mathrm{d}t} = -v_a \frac{\mathbf{B}_i}{\|\mathbf{B}_i\|} \tag{19}$$

where $\mathbf{B}_i$ is direction of movement of ith mobile agent. This is analogous to the ansatz used here, and as we explain below, $\mathbf{B}_i$ is also a gradient of a function.

The SMC coverage is defined as a distribution

$$c_{\text{smc}}(\mathbf{x}) = \frac{1}{N\,t}\sum_{i=1}^{N}\int_0^t \delta(\mathbf{x}-\mathbf{z}_i(\tau))\,\mathrm{d}\tau \tag{20}$$

where $\delta(x)$ is the Dirac delta function. The coverage defined in (4) has a clear connection to (20). Since the coverage c_σ depends on the choice of the RBF, we need to guarantee some sensible representation of ϕ in the limit. Therefore, ϕ must be a standard mollifier function that satisfies

$$\lim_{\sigma\to 0}\phi_\sigma(\mathbf{x}) = \lim_{\sigma\to 0}\sigma^{-n}\phi\left(\frac{\mathbf{x}}{\sigma}\right) = \delta(\mathbf{x}). \tag{21}$$

If we let $\sigma \to 0$ the relative coverage function will became a distribution

$$\lim_{\sigma\to 0} c_\sigma(\mathbf{x}) = c_{\text{smc}}(\mathbf{x}) \tag{22}$$

and smoothing of goal density is diminished

$$\lim_{\sigma\to 0}(\phi_\sigma * m)(\mathbf{x}) = m(\mathbf{x}). \tag{23}$$

Similar to (7), in [26] an appropriate, smoothing, norm E_{smc} was defined in order to quantify how well the trajectories of agents are sampling a given goal coverage m

$$E_{\text{smc}}(t) = \|c_{\text{smc}} - m\|^2_{H^{-\frac{n+1}{2}}} = \sum_{k\in Z^{*n}}\Lambda(\mathbf{k})|c_{\mathbf{k}} - m_{\mathbf{k}}|^2 \tag{24}$$

where $c_{\mathbf{k}}$ and $m_{\mathbf{k}}$ are the Fourier coefficients of c_{smc} and m, respectively. Furthermore, $\Lambda(\mathbf{k})$ is defined as

$$\Lambda(\mathbf{k}) = \frac{1}{\left(1+\|\mathbf{k}\|^2\right)^{\frac{n+1}{2}}} \tag{25}$$

which is used as a scale factor that gives greater influence of large-scale modes than the small-scale modes. The role of Λ scaling is similar to the role of the heat equation in the HEDAC model, because it provides a smoothing effect on the spatial error.

The norm E_{smc} measures the distance between c_{smc} and m as given by the Sobolev space norm of negative index and it quantifies how much the time averages of the Fourier basis functions deviate from their spatial averages. From (22) and (23), it can be seen that for a small σ the coverage c_σ and $\phi_\sigma * m$ are reasonable approximations of c_{smc} and m, respectively. For a small σ it is possible to compare the convergence results for SMC and HEDAC algorithms using norms (7) or (24).

A feedback control is designed to manage the movement of agents using the gradient method that minimizes the E_{smc} for small time step Δt. The ith agent's direction is calculated as

$$\mathbf{B}_i(t) = \sum_k \Lambda(\mathbf{k})(c_{\mathbf{k}} - m_{\mathbf{k}})\nabla f_{\mathbf{k}}(\mathbf{z}_i(t)) \tag{26}$$

where $f_{\mathbf{k}}$ are the Fourier basis functions that satisfy the Neumann boundary condition. For a 2-D implementation of SMC algorithm, Fourier basis functions are calculated on a rectangular domain $[0, L_1]\times[0, L_2]$ as

$$f_{\mathbf{k}}(\mathbf{x}) = \frac{1}{h_{\mathbf{k}}}\cos\left(\frac{k_1\pi x_1}{L_1}\right)\cos\left(\frac{k_2\pi x_2}{L_2}\right)$$
$$h_{\mathbf{k}} = \int_0^{L_1}\int_0^{L_2}\cos^2\left(\frac{k_1\pi x_1}{L_1}\right)\cos^2\left(\frac{k_2\pi x_2}{L_2}\right)\mathrm{d}x_1\,\mathrm{d}x_2 \tag{27}$$

where $\mathbf{k} = (k_1, k_2)$ is the wave-number vector. The cosine basis functions satisfy the Neumann boundary condition

$$\frac{\partial f_{\mathbf{k}}}{\partial \mathbf{n}} = 0, \text{ on } \partial\Omega. \tag{28}$$

B. Implementation of HEDAC Using Fourier Series Method

Although the finite differences will be used primarily, the solution to (11) with Neumann boundary condition can be found using a 2-D Fourier series. Let us assume that the domain Ω is a $[0, L_1]\times[0, L_2]$ rectangle and let us extend the temperature field u and source s to be even and periodic functions in both spatial directions. Functions a and s can be represented as a Fourier series

$$s(\mathbf{x}) = \sum_{\mathbf{k}} s_{\mathbf{k}} f_{\mathbf{k}},\ a(\mathbf{x}) = \sum_{\mathbf{k}} a_{\mathbf{k}} f_{\mathbf{k}} \tag{29}$$

where $\mathbf{k} = (k_1, k_2)$ is the wave-number vector and $f_{\mathbf{k}}$ defined in (27) satisfies the Neumann boundary condition (12). Using (11), we get

$$u(\mathbf{x}) = \sum_{\mathbf{k}} u_{\mathbf{k}} f_{\mathbf{k}} \tag{30}$$

$$u_{\mathbf{k}} = \frac{s_{\mathbf{k}} - \gamma a_{\mathbf{k}}}{\beta + \alpha\mathbf{k}^2}. \tag{31}$$

From (30) and (31), the gradient of u can be expressed using Fourier series

$$\nabla u(\mathbf{x}) = \sum_k \frac{s_{\mathbf{k}} - \gamma a_{\mathbf{k}}}{\beta + \alpha\mathbf{k}^2}\nabla f_{\mathbf{k}}(\mathbf{x}). \tag{32}$$

Note that the formulation of the agent control in (32) and (26) are very similar. In fact, if we set $\gamma = 0$ we can see in (32) that the role of the denominator is to provide scaling of higher Fourier coefficients. This scaling produces a smoothing effect on the field s that is very similar to the scaling in (26).

IV. Area Coverage Simulations

The proposed method is implemented for a 2-D area coverage problem for conducting coverage simulations. The heat equation is solved using implicit finite difference scheme on uniform orthogonal mesh. From the obtained solution, i.e., temperature field, a gradient ∇u is interpolated using bilinear interpolation. For the numerical tests presented in the following section, the Gaussian function is used as RBF. The goal density discretization $\mathbf{m}$ and coverage discretization $\mathbf{c}$ are calculated with standard deviation σ and local cooling $\mathbf{a}$ with σ_a. Euler's method is utilized to solve agent motion equation (9).

Testing of the proposed method is conducted on a several examples designed to reveal the behavior of the multiagent system in different conditions such as different domain size

and agents properties. All the test cases are 2-D area coverage problems with given smooth or nonsmooth goal density fields. Different HEDAC parameters are used to provide agent behavior in accordance with the given test case.

In order to compare SMC and HEDAC algorithms, we used the SMC algorithm with $\phi_\sigma * m$ and c_σ instead of standard m and c_{smc}, respectively. This modification allows the use of fast fourier transform (FFT) which provides a much faster computation. The modification was thoroughly tested and showed no significant difference in terms of convergence or overall performance.

The results of simulations for the described test cases are presented in figures described below and video animations available as supplemental material. The video animations, labeled as videos 1–3, show the trajectories of agents along with fields: goal density m, coverage density c_σ, source s, and temperature u. The error E, defined in (7), is also plotted. The animations are based on coverage simulations with given agents' initial position, as defined in the description of each test case.

To show and compare the convergence of HEDAC and SMC methods independent on the choice of agent initial positions, we performed Monte Carlo simulations with random initial location of agents. For each test case, total of 100 coverage simulations are conducted where agents are initially positioned randomly within the part of the domain where $m > 0$. For each simulation two different error formulations are observed: E and E_{smc} as defined in (7) and (24), respectively.

A. Test 1

In the first test case we consider a coverage of a rectangulary shaped area with uniform density m (gray area in Fig. 1). The Gaussian RBS ϕ_σ has standard deviation $\sigma = 1$.

For solving the stationary heat equation (11) by finite differences, the domain is discretized to 250×250 uniform grid. For the heat equation parameters we used $\alpha = 0.02$ and $\beta = 2{\cdot}10^{-4}$ ($\beta_0 = 2$) reflecting the very simple shape of the goal density.

Five agents were used for coverage simulations with velocity $v_a = 2$. Agent's cooling is controlled with $\gamma = 1{\cdot}10^{-6}$ ($\gamma_0 = 0.01$) and $\sigma_a = 1$. Initial positions of five agents are: $(20, 56)$, $(35, 53)$, $(50, 50)$, $(65, 47)$, and $(80, 44)$. test 1 is computed on a time interval $[0, 1000]$ with the time step $\Delta t = 0.2$. The results of area coverage for this test, presented as agent trajectories, are shown in Fig. 1. Paths of agents are plotted for two different times: $t = 200$ and $t = 1000$.

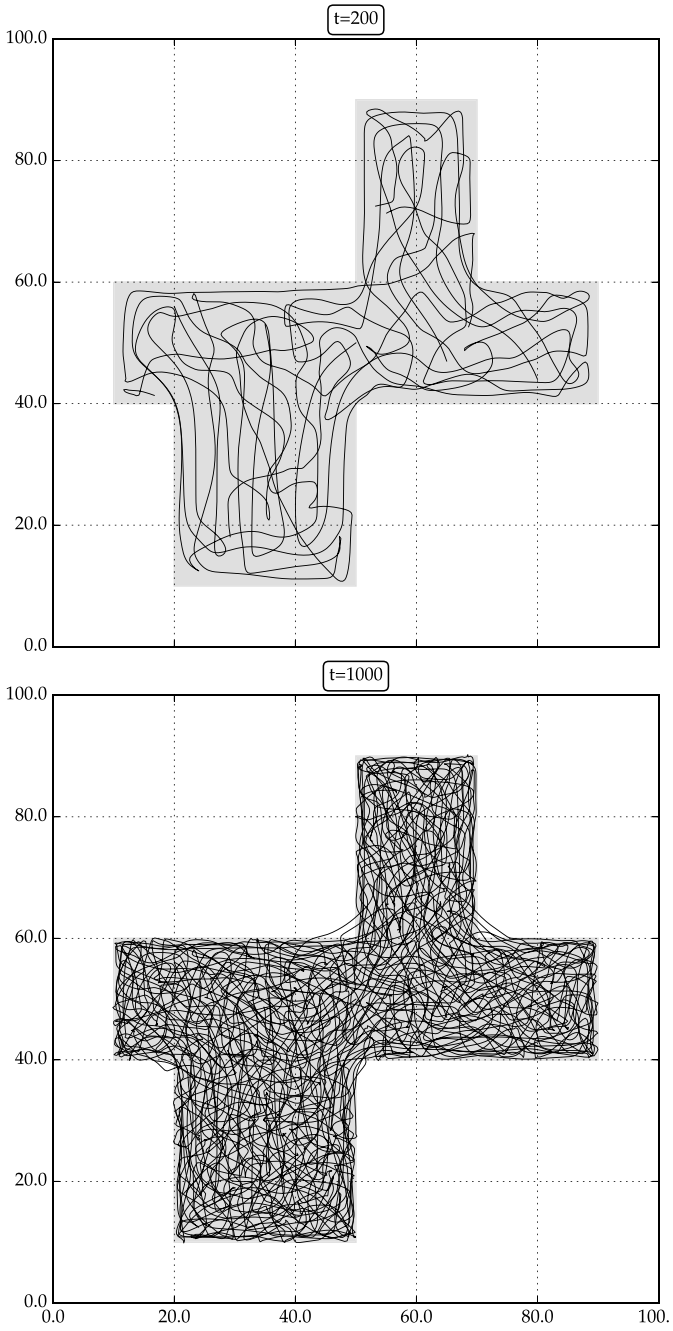

Fig. 1. Test 1: agents paths using HEDAC coverage algorithm at $t = 200$ and $t = 1000$, with 250×250 uniform grid, the time step $\Delta t = 0.2$ and parameters $\alpha = 0.02$, $\beta = 2 \cdot 10^{-4}$ ($\beta_0 = 2$), $\gamma = 1 \cdot 10^{-6}$ ($\gamma_0 = 0.01$), $v_a = 2$, and $\sigma_a = \sigma = 1$.

As is evident from Fig. 1, by the end of the simulation the area of interest is comprehensively and uniformly covered with agents trajectories. The trajectories are smooth, and there is no evidence of a numerical instability in terms of glitches or deadlocks. This indicates that temperature field u is changing smoothly in both time and space and provides stable agent guidance trough its gradient. The dynamics of agents movement can be more closely observed in video 1.

In Fig. 2, agent trajectories achieved with SMC are plotted for time $t = 1000$ which can be compared with second subplot in Fig. 1. As discussed above, the SMC trajectories initially explore large scales due to the algorithm's dependence on the global, Fourier representation. Due to the local nature of the field of functions $\phi_\sigma^{\mathbf{x}}$ HEDAC produces a more uniform coverage and stays more closely within the boundaries of the goal density.

Comparison of evaluated errors is shown in Fig. 3 where the average errors (for 100 runs) are plotted. As is seen from the plot of E versus time, HEDAC has a better convergence than SMC after about $t = 10$. This is expected, due to the local nature of both measure of convergence and HEDAC algorithm. For E_{smc} the situation is different. At the beginning of

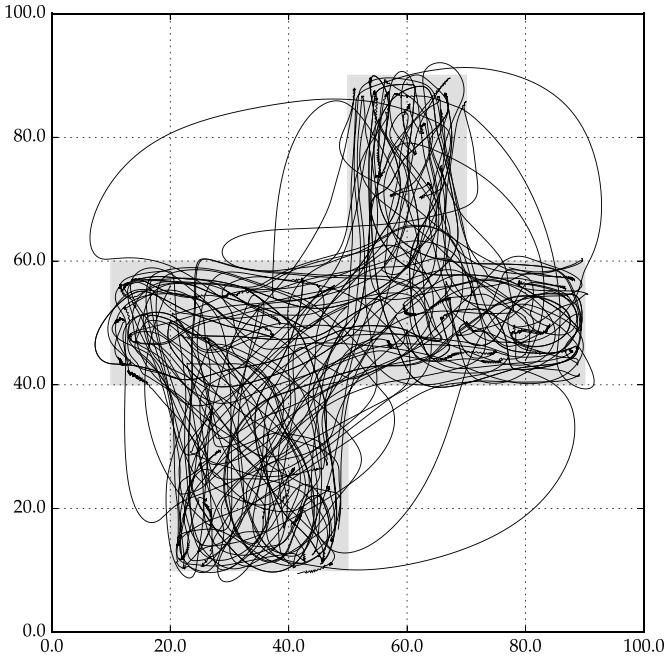

Fig. 2. Test 1: agents paths using SMC algorithm at $t = 1000$ with 250×250 uniform grid, time step $\Delta t = 0.2$ and parameters $v_a = 2$ and $\sigma_a = \sigma = 1$.

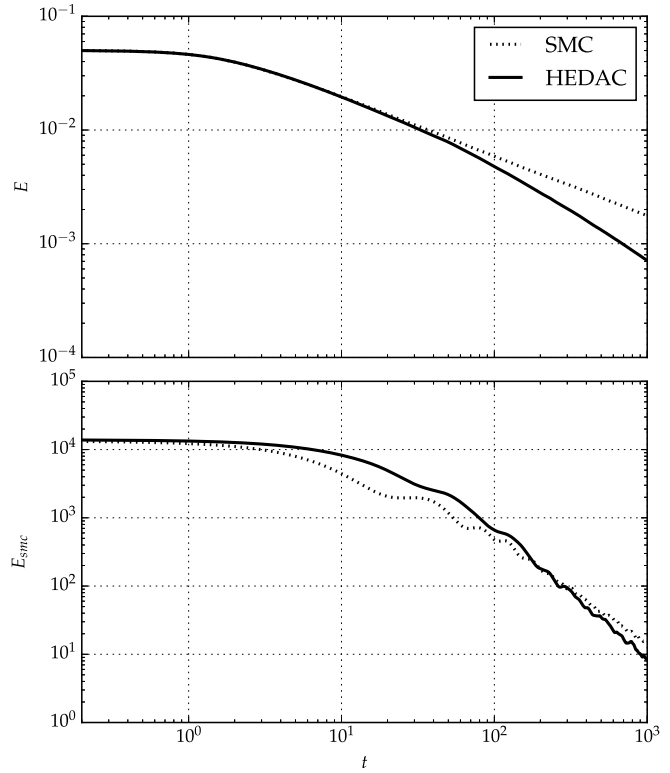

Fig. 3. Test 1: the convergence of HEDAC and SMC algorithms with averaged errors E and E_{smc} based on 100 runs with random agent initial positions. The slope of almost straight lines on log–log scale shows the $\mathcal{O}(t^{-1})$ convergence rate.

the coverage process, SMC directs agents to ensure a global coverage in term of matching the lower Fourier coefficients m_k and c_k in (24). This is achieved by scaling the Fourier

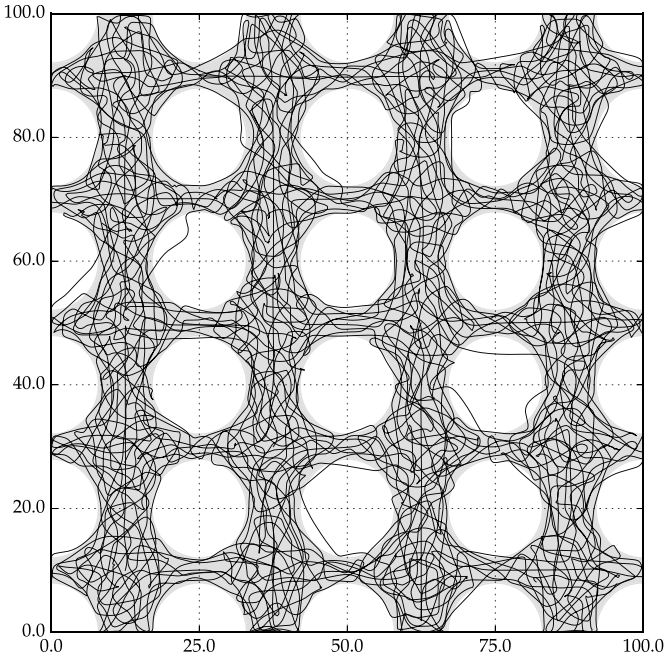

Fig. 4. Test 2: agents paths using HEDAC coverage algorithm at $t = 1000$, with 400×400 uniform grid, the time step $\Delta t = 0.2$ and parameters $\alpha = 2 \cdot 10^{-3}$, $\beta = 1 \cdot 10^{-4}$ ($\beta_0 = 1$), $\gamma = 1 \cdot 10^{-6}$ ($\gamma_0 = 0.01$), $v_a = 2$, and $\sigma_a = \sigma = 1$.

coefficient with $\Lambda(k)$. In later times, when matching of lower coefficients is achieved, the agents movement is dominantly controlled by the difference of higher Fourier coefficients of trajectories and the goal density. As both E_{smc} norm and the SMC algorithm are based on same scaling of Fourier coefficients, it is reasonable to expect that SMC will yield better results in E_{smc} norm than HEDAC. But, due to a focus on a global coverage at the beginning, which does not take smaller scale aspects into account, the forthcoming convergence of E_{smc} is weakened. Thus, eventually, and as expected due to its focus on local features, the HEDAC algorithm outperforms SMC also in terms of the E_{smc} norm.

B. Test 2

The second test case has a more complex structure of the goal density, where area of interest covers the whole domain excluding circular patches (Fig. 4). This test is designed to examine the behavior of agent movement on the "porous" goal density, where it is preferable that agents avoid passing over areas of zero interest. This test also shows the behavior of agents near the boundary of the domain.

A 400×400 uniform grid is used for solving the heat equation specified by the diffusion rate $\alpha = 2 \cdot 10^{-3}$ and the convective cooling coefficient $\beta = 1 \cdot 10^{-4}$ ($\beta_0 = 1$). Compared with the first test case, a weaker conductive heat transfer and stronger convective cooling are used in order to achieve more detailed and localized movement. Used numerical mesh is denser to allow for more precise and detailed reconstruction of the goal density, coverage density and consequentially temperature fields. Standard deviation $\sigma = 1$ is used in ϕ_σ.

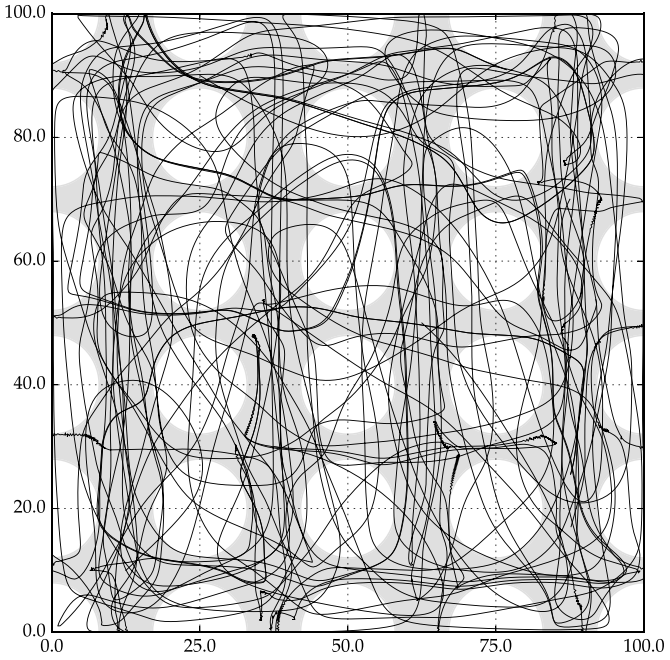

Fig. 5. Test 2: agents paths using SMC algorithm at $t = 1000$ with 400×400 uniform grid, time step $\Delta t = 0.2$ and parameters $v_a = 2$ and $\sigma_a = \sigma = 1$.

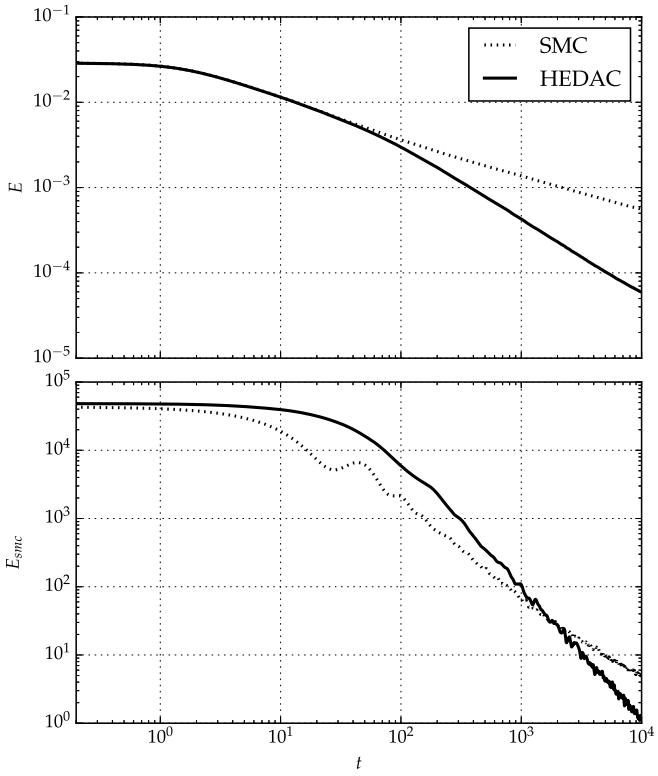

Fig. 6. Test 2: the convergence of HEDAC and SMC algorithms with averaged errors E and E_{smc} based on 100 runs with random agent initial positions. The slope of almost straight lines on log–log scale shows the $\mathcal{O}(t^{-1})$ convergence rate.

The simulation of the coverage using six agents is conducted on the time interval $[0, 1000]$ with the time step $\Delta t = 0.2$. Initial position of agents are given by: $(12.5, 10)$, $(37.5, 30)$, $(62.5, 50)$, $(87.5, 70)$, $(12.5, 90)$, and $(25, 90)$. The agents' velocity is $v_a = 2$ and the local cooling parameters are $\gamma = 1 \cdot 10^{-6}$ ($\gamma_0 = 0.01$) and $\sigma_a = 1$.

The results of the second test are shown in Fig. 4. Again, as in the first test case, trajectories uniformly cover the area of interest and passing trough the area of no interest is negligible both in terms of occurrences and in the length of trajectories outside of the area of interest.

From presented results, agents are very often near the boundary of the domain where their behavior is very stable without any glitches or deadlocks. It can be concluded that the use of Neumann boundary condition (12) in combination with gradient interpolation is suitable for handling agent's behavior near the boundary.

The SMC has excessive passing over circular patches where no coverage is needed (Fig. 5). This is due to the fact that properly adapted SMC would in this case—instead of the Fourier basis—require bases functions that are adapted to the goal density—in particular the basis functions would have to be zero on the inside of the excluded zones. Such a basis would have to solve

$$\triangle f_k = \lambda_k f_k$$

on the gray area. But changing the basis for every goal density is cumbersome. HEDAC resolves this by using a nonadapted RBF family of functions.

For better comparison of long term convergence, the duration of coverage simulation is prolonged up to $t = 10000$. Plots of errors over time are shown in Fig. 6. The behavior of the errors is very similar to the test 1, where HEDAC outperforms SMC over longer times in both norms.

C. Test 3

The third test is designed to show performance of HEDAC method with a larger swarm of agents with continuous goal density function given as

$$m(x) = \frac{\sin^2(x_1 - \pi)\sin^2(x_2 - \pi) + 0.1 \cdot \sin\left(\frac{x_1 \cdot x_2 \cdot \pi}{2}\right)}{\cos\left(\frac{x_1 \cdot x_2 \cdot \pi}{2}\right) + 2}. \quad (33)$$

The coverage is simulated with the use of 20 agents over a $[2\pi \times 2\pi]$ domain. The simulation is conducted for agents initially positioned on a grid layout $(0.3\pi, 0.65\pi, 1.0\pi, 1.35\pi, 1.7\pi) \times (3/6\pi, 5/6\pi, 7/6\pi, 9/6\pi)$ for time $t \in [0, 100]$. A 500×500 uniform rectangular numerical grid and the time step $\Delta t = 0.02$ are used for this case.

The parameters of the heat equation are as follows: $\alpha = 0.025$ and $\beta = 2.533$ ($\beta_0 = 100$). The Gaussian RBF is used with the standard deviation $\sigma = 0.01 \cdot \pi$ for goal and coverage density fields, and $\sigma_a = 0.02 \cdot \pi$ for local cooling. Agent behavior parameters are $\gamma = 2.533 \cdot 10^{-4}$ ($\gamma_0 = 0.01$) and $v_a = 1$. As large number of agents are used, both convective and agents cooling is increased to achieve better cooperation and thorough local search.

This test uses a swarm of agents on a longer time scale, hence the trajectories are very dense and impractical to show.

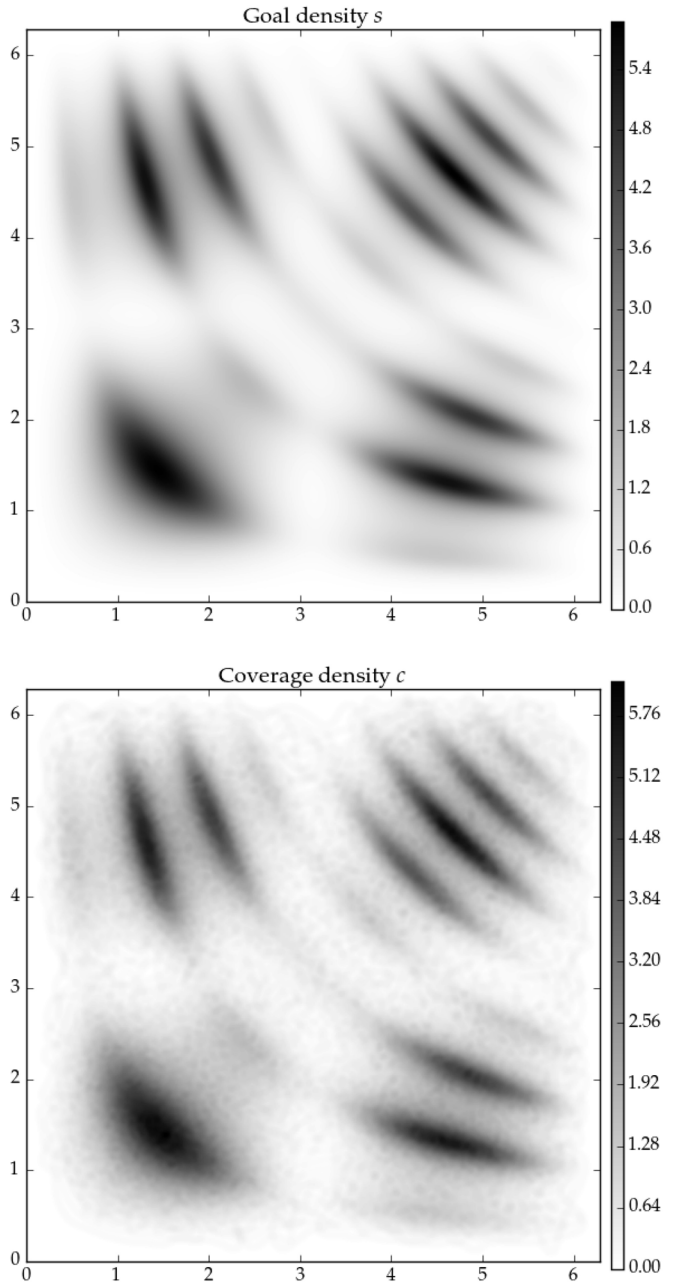

Fig. 7. Test 3: goal and HEDAC coverage density fields at $t = 100$ with 500×500 uniform grid, the time step $\Delta t = 0.02$ and parameters $\alpha = 0.025$, $\beta = 2.533$ ($\beta_0 = 100$), $\gamma = 2.533 \cdot 10^{-4}$ ($\gamma_0 = 0.01$), $v_a = 1$, and $\sigma_a = \sigma = 0.02 \cdot \pi$.

The final results of the coverage simulation for test 3 are displayed in Fig. 7 as plot of the coverage density c_σ which can be compared with the plot of the goal density $\phi_\sigma * m$. A detailed matching of coverage and goal density fields is reached, which shows competence and efficiency of the HEDAC method for solving this class of problems.

This presentation of coverage simulation results emphasizes the choice of standard deviation σ used in Gaussian RBF. The thickness of agent trails, regulated by σ, is visible in the coverage plot. Use of other σ would yield a dissimilar behavior of agents and consequentially different overall coverage strategy with various movement patterns.

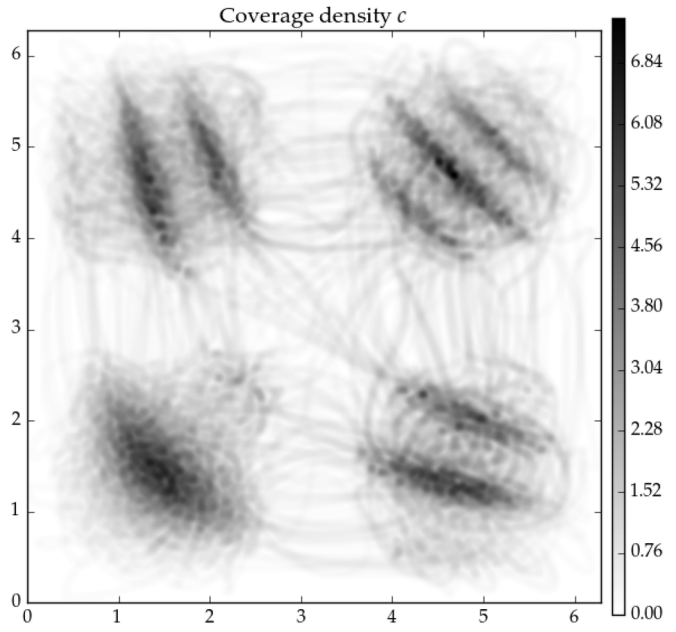

Fig. 8. Test 3: coverage density using SMC algorithm at $t = 100$ with 500×500 uniform grid, time step $\Delta t = 0.02$ and parameters $v_a = 1$ and $\sigma_a = \sigma = 0.02 \cdot \pi$.

The coverage density obtained with SMC is displayed in Fig. 8 and it can be compared with goal and coverage density plots in Fig. 7. HEDAC produces smoother coverage with more precise matching to the local shape of the goal density, while the SMC showed high disparity of coverage compared with details of the goal field. This conclusion is confirmed by the convergence result for error E in Fig. 9. On the other hand, when comparing the error and convergence in the E_{smc} norm it is seen that SMC provides a better coverage of the large-scale features of the goal density.

D. Remarks on Convergence

Different convergence results in Figs. 3, 6, and 9 are shown on a log–log scale. These plots clearly indicate that the sampling error HEDAC is roughly $\mathcal{O}(t^{-1})$. This is similar to quasi-Monte Carlo sampling which has error $\mathcal{O}(t^{-1})$ as opposed to regular Monte Carlo sampling which has error $\mathcal{O}(t^{-1/2})$ (here, of course, time t plays the role of number of samples). This is not surprising because quasi-Monte Carlo methods are based on low-discrepancy sequences and similarly the SMC and HEADAC algorithms attempt to generate points on agent trajectories such that they have density proportional to m throughout the domain.

E. Computational Efficiency

We used the previously given coverage test cases to measure and compare the computational efficiency of HEDAC and SMC coverage algorithm implementations. For this purpose, the implementation of algorithms were modified in such a way that all the unnecessary computational procedures (E and E_{smc} calculation, visualizations and the results saving) are omitted from both coverage methods.

TABLE I
COMPUTATIONAL EFFICIENCY COMPARISON: HEDAC VERSUS SMC COMPUTATIONAL TIMES

	Algorithm		Tests		
			Test 1	Test 2	Test 3
		Mesh size	250×250	400×400	500×500
		No. of time steps	5000	5000	5000
		No. of agents	5	6	20
Computational time [s]	HEDAC	Initialization	2.17	6.33	10.84
		Simulation	593.1	1553.7	6270.2
		Time step	0.119	0.311	1.254
	SMC	Initialization	0.05	0.11	0.05
		Simulation	677.5	1827.1	7396.8
		Time step	0.136	0.365	1.479

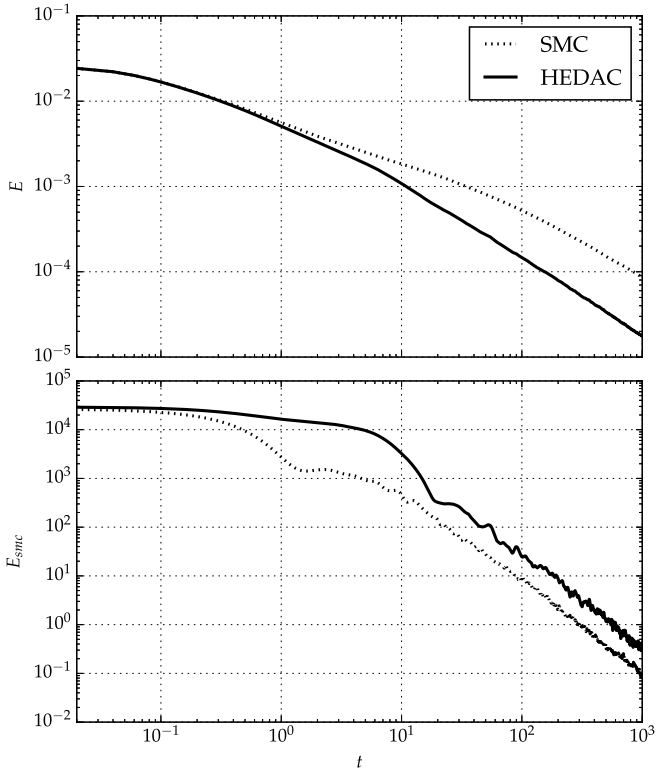

Fig. 9. Test 3: the convergence of HEDAC and SMC algorithms with averaged errors E and E_{smc} based on 100 runs with random agent initial positions. The slope of almost straight lines on log–log scale shows the $\mathcal{O}(t^{-1})$ convergence rate.

The test recorded the initialization time and the time needed to conduct all coverage simulation time steps, separately. Initialization covers data preparation, domain discretization and, in HEDAC, formation of the sparse linear system and the LU decomposition. The simulation time covers the main time stepping loop, which consists of several demanding computations: the Euler method for solving for the motion of agents, solving the differential heat equation (HEDAC) and FFT (SMC). The simulations are performed on 3.4 GHz Intel Core i7 workstation. To obtain the computational times, simulations of all three tests with both methods were conducted. Each simulation was repeated ten times and the average computational times are given in Table I.

It can be observed that, in terms of computational performance, HEDAC is competitive with SMC. Although slower in initialization, the implementation of HEDAC is faster in calculation of each time step. Based on the computational times for a relatively dense spatial discretization, we believe that HEDAC could even be suitable for real-time calculations and planning of area coverage where period between control decisions is more than several seconds.

V. CONCLUSION

In this paper, we have introduced a new multiagent centralized feedback control method for area coverage based on a combination of techniques from potential field approaches and ergodicity approaches. The presented method can be used for solving multidimensional coverage problems.

The behavior of the HEDAC algorithm is demonstrated on three 2-D area coverage test cases and results are visually presented, analyzed and compared with SMC. Test cases are designed to show a behavior of multiagent coverage in different conditions. Very good results are achieved in all conducted tests, showing superiority of the presented method for area coverage applications that have complex local features.

The numerical implementation of HEDAC is relatively simple. The algorithm is robust, fast, and scalable, and it offers a possibility of fine tuning through several parameters of the method. The problem of cooperation and coordination of multiagent system is built in organically via RBFs. Collision and deadlock avoidance is successfully achieved through the formulation of source and local cooling terms and no occurrences of instabilities of any kind are recorded.

The mathematical theory behind integral components of HEDAC method is relatively well known and this gives solid base for more detailed overall theoretical investigations of the method. Although the HEDAC algorithm converges smoothly in all performed tests, proving convergence remains an open challenge.

There are many possibilities to improve and extend the HEDAC algorithm and to adapt it for application to other related problems. The algorithm can be adapted for decentralized coverage using techniques developed in [34] and [41] or

by using several heat equations for several connected groups of agents.

For the real world applications, second order motion control or even more detailed motion model with realistic limitations can be introduced. The method can be applied to achieve various goals based on continuous autonomous movement over a certain area such as: surveillance and inspection missions, planing of search-and-rescue, various data acquisition, or other autonomous actions like cleaning or painting.

REFERENCES

[1] E. U. Acar and H. Choset, "Robust sensor-based coverage of unstructured environments," in *Proc. IEEE/RSJ Int. Conf. Intell. Robots Syst.*, vol. 1. 2001, pp. 61–68.

[2] E. U. Acar and H. Choset, "Sensor-based coverage of unknown environments: Incremental construction of Morse decompositions," *Int. J. Robot. Res.*, vol. 21, no. 4, pp. 345–366, 2002.

[3] J. J. Acevedo, B. C. Arrue, I. Maza, and A. Ollero, "Cooperative large area surveillance with a team of aerial mobile robots for long endurance missions," *J. Intell. Robot. Syst.*, vol. 70, nos. 1–4, pp. 329–345, 2013.

[4] A. Ahmadzadeh, "Cooperative control of UAVs for search and coverage," in *Proc. AUVSI Conf. Unmanned Syst.*, Orlando, FL, USA, 2006, pp. 1–14.

[5] A. Ahmadzadeh, A. Jadbabaie, V. Kumar, and G. J. Pappas, "Cooperative coverage using receding horizon control," in *Proc. Eur. Control Conf.*, 2007, pp. 2466–2470.

[6] D. D. Bochtis and T. Oksanen, "Combined coverage and path planning for field operations," in *Proc. 7th Eur. Conf. Precision Agr.*, Wageningen, The Netherlands, 2009, pp. 521–527.

[7] H. Choset, "Coverage for robotics—A survey of recent results," *Ann. Math. Artif. Intell.*, vol. 31, nos. 1–4, pp. 113–126, 2001.

[8] J. Cortes, S. Martinez, T. Karatas, and F. Bullo, "Coverage control for mobile sensing networks," *IEEE Trans. Robot. Autom.*, vol. 20, no. 2, pp. 243–255, Apr. 2004.

[9] R. Daily and D. M. Bevly, "Harmonic potential field path planning for high speed vehicles," in *Proc. IEEE Amer. Control Conf.*, Seattle, WA, USA, 2008, pp. 4609–4614.

[10] C. Franco, G. López-Nicolás, C. Sagüés, and S. Llorente, "Adaptive action for multi-agent persistent coverage," *Asian J. Control*, vol. 18, no. 2, pp. 419–432, 2015.

[11] C. Franco, D. M. Stipanović, G. López-Nicolás, C. Sagüés, and S. Llorente, "Persistent coverage control for a team of agents with collision avoidance," *Eur. J. Control*, vol. 22, pp. 30–45, Mar. 2015.

[12] Y. Gabriely and E. Rimon, "Spanning-tree based coverage of continuous areas by a mobile robot," *Ann. Math. Artif. Intell.*, vol. 31, nos. 1–4, pp. 77–98, 2001.

[13] E. Garcia and P. Gonzalez De Santos, "Mobile-robot navigation with complete coverage of unstructured environments," *Robot. Autonom. Syst.*, vol. 46, no. 4, pp. 195–204, 2004.

[14] P. Grisvard, *Elliptic Problems in Nonsmooth Domains* (Monographs and Studies in Mathematics, 24). Boston, MA, USA: Pitman Adv. Program, 1985.

[15] P. F. Hokayem, D. Stipanović, and M. W. Spong, "Dynamic coverage control with limited communication," in *Proc. IEEE Amer. Control Conf. (ACC)*, New York, NY, USA, 2007, pp. 4878–4883.

[16] A. Howard, M. J. Matarić, and G. S. Sukhatme, "Mobile sensor network deployment using potential fields: A distributed, scalable solution to the area coverage problem," in *Distributed Autonomous Robotic Systems 5*. Tokyo, Japan: Springer, 2002, pp. 299–308.

[17] A. Hubenko, V. A. Fonoberov, G. Mathew, and I. Mezić, "Multiscale adaptive search," *IEEE Trans. Syst., Man, Cybern. B, Cybern.*, vol. 41, no. 4, pp. 1076–1087, Aug. 2011.

[18] I. I. Hussein and D. M. Stipanovic, "Effective coverage control for mobile sensor networks with guaranteed collision avoidance," *IEEE Trans. Control Syst. Technol.*, vol. 15, no. 4, pp. 642–657, Jul. 2007.

[19] A. Khan, E. Yanmaz, and B. Rinner, "Information merging in multi-UAV cooperative search," in *Proc. IEEE Int. Conf. Robot. Autom. (ICRA)*, Hong Kong, 2014, pp. 3122–3129.

[20] B. O. Koopman, "The theory of search: III. The optimum distribution of searching effort," *Oper. Res.*, vol. 5, no. 5, pp. 613–626, 1957.

[21] B. O. Koopman, "The theory of search. I. Kinematic bases," *Oper. Res.*, vol. 4, no. 3, pp. 324–346, 1956.

[22] B. O. Koopman, "The theory of search. II. Target detection," *Oper. Res.*, vol. 4, no. 5, pp. 503–531, 1956.

[23] O.-A. Ladyzhenskaya, N.-N. Ural'tseva, and L. Ehrenpreis, *Linear and Quasilinear Elliptic Equations*. New York, NY, USA: Academic Press, 1968.

[24] E. Masehian and M. R. Amin-Naseri, "A voronoi diagram-visibility graph-potential field compound algorithm for robot path planning," *J. Robot. Syst.*, vol. 21, no. 6, pp. 275–300, 2004.

[25] A. A. Masoud, "A harmonic potential field approach for joint planning and control of a rigid, separable nonholonomic, mobile robot," *Robot. Autonom. Syst.*, vol. 61, no. 6, pp. 593–615, 2013.

[26] G. Mathew and I. Mezic, "Spectral multiscale coverage: A uniform coverage algorithm for mobile sensor networks," in *Proc. 48th IEEE Conf. Decis. Control Held Jointly 28th Chin. Control Conf. (CDC/CCC)*, Shanghai, China, 2009, pp. 7872–7877.

[27] G. Mathew and I. Mezić, "Metrics for ergodicity and design of ergodic dynamics for multi-agent systems," *Phys. D Nonlin. Phenom.*, vol. 240, nos. 4–5, pp. 432–442, 2011.

[28] G. Mathew, A. Surana, and I. Mezić, "Uniform coverage control of mobile sensor networks for dynamic target detection," in *Proc. 49th IEEE Conf. Decis. Control (CDC)*, Atlanta, GA, USA, 2010, pp. 7292–7299.

[29] R. J. Meuth, E. W. Saad, D. C. Wunsch, and J. Vian, "Adaptive task allocation for search area coverage," in *Proc. IEEE Int. Conf. Technol. Pract. Robot Appl. (TePRA)*, Woburn, MA, USA, 2009, pp. 67–74.

[30] A. Renzaglia and A. Martinelli, "Potential field based approach for coordinate exploration with a multi-robot team," in *Proc. IEEE Int. Workshop Safety Security Rescue Robot. (SSRR)*, Bremen, Germany, 2010, pp. 1–6.

[31] S. A. Sadat, J. Wawerla, and R. T. Vaughan, "Recursive non-uniform coverage of unknown terrains for UAVs," in *Proc. IEEE/RSJ Int. Conf. Intell. Robots Syst. (IROS)*, Chicago, IL, USA, 2014, pp. 1742–1747.

[32] K. Sato, "Deadlock-free motion planning using the laplace potential field," *Adv. Robot.*, vol. 7, no. 5, pp. 449–461, 1992.

[33] A. Saudi and J. Sulaiman, "Path planning for mobile robot with half-sweep successive over-relaxation (HSSOR) iterative method," in *Proc. Symp. Progress Inf. Commun. Technol. (SPICT)*, Kuala Lumpur, Malaysia, 2009, pp. 57–62.

[34] C. Song, G. Feng, Y. Fan, and Y. Wang, "Decentralized adaptive awareness coverage control for multi-agent networks," *Automatica*, vol. 47, no. 12, pp. 2749–2756, 2011.

[35] A. Spira1, N. Sochen, and R. Kimmel, "Geometric filters, diffusion flows, and kernels in image processing," in *Handbook of Geometric Computing*. Heidelberg, Germany: Springer, 2005, pp. 203–230.

[36] L. D. Stone, *Theory of Optimal Search*. New York, NY, USA: Academic Press, 1975.

[37] A. Surana, G. Mathew, and S. Kannan, "Coverage control of mobile sensors for adaptive search of unknown number of targets," in *Proc. IEEE Int. Conf. Robot. Autom. (ICRA)*, St. Paul, MN, USA, 2012, pp. 663–670.

[38] P. Vadakkepat, K. C. Tan, and W. Ming-Liang, "Evolutionary artificial potential fields and their application in real time robot path planning," in *Proc. Congr. Evol. Comput.*, vol. 1. 2000, pp. 256–263.

[39] J. Wood and J. K. Hedrick, "Space partitioning and classification for multi-target search and tracking by heterogeneous unmanned aerial system teams," in *Proc. Infotech Aerosp.*, St. Louis, MO, USA, 2011, p. 1443.

[40] Y. Yang, M. M. Polycarpou, and A. A. Minai, "Multi-UAV cooperative search using an opportunistic learning method," *J. Dyn. Syst. Meas. Control*, vol. 129, no. 5, pp. 716–728, 2007.

[41] C. Zhai and Y. Hong, "Decentralized sweep coverage algorithm for multi-agent systems with workload uncertainties," *Automatica*, vol. 49, no. 7, pp. 2154–2159, 2013.

Authors' photographs and biographies not available at the time of publication.